Control of free vibration with piezoelectric materials: Finite element modeling based on Timoshenko beam theory

Myung-Kwan Song†

Department of Civil Engineering, The University of Tokyo, Tokyo 113-8656, Japan

Hyuk-Chun Noh‡

Department of Civil Engineering and Engineering Mechanics, Columbia University, New York, NY 10027, U.S.A.

Sun-Hoon Kim‡†

Department of Civil Engineering, Youngdong University, Chungbuk 370-701, Korea

In-Seon Han‡‡

Department of Civil and Environmental Engineering, Korea Advanced Institute of Science and Technology, Daejeon 305-701, Korea

Abstract.   In this study, a new smart beam finite element is proposed for the finite element modeling of beam-type smart structures that are equipped with bonded plate-type piezoelectric sensors and actuators. Constitutive equations for the direct piezoelectric effect and converse piezoelectric effect of piezoelectric materials are considered in the formulation. By using a variational principle, the equations of motion for the smart beam finite element are derived. The proposed 2-node beam finite element is an isoparametric element based on Timoshenko beam theory. The proposed smart beam finite element is applied to the free vibration control adopting a constant gain feedback scheme. The electrical force vector, which is obtained in deriving an equation of motion, is the control force equivalent to that in existing literature. Validity of the proposed element is shown through comparing the analytical results of the verification examples with those of other previous researchers. With the use of smart beam finite elements, simulation of free vibration control is demonstrated by sensing the voltage of the piezoelectric sensors and by applying the voltages to the piezoelectric actuators.

Key words: piezoelectric materials; piezoelectric sensor; piezoelectric actuator; Timoshenko beam theory; free vibration control.

† Postdoctoral Researcher
‡ Research Associate
‡† Associate Professor, Corresponding author, E-mail: kimsh@youngdong.ac.kr
‡‡ Ph.D. Candidate

1. Introduction

Smart materials behave as organisms in that they comply with the surrounding environment, in which they are placed. Engineering structures equipped with these materials can perceive changes in their environment, possesses the ability to recover from damages, and decide the length of their own life, etc., thereby maximizing the monitoring effect. They can also improve the stability, health, and reliability of engineering structures. It is expected that protection of structural life and property from unpredictable disasters is possible with the application of smart structures in various fields of civil engineering. In addition, if health monitoring is possible with the damage predicting sensors, life cycle-costs can be reduced since the length of structure's life is increased, especially for cases where connections of beams and columns are hidden. Smart materials are also advantageous for use in underground structures, underwater structures, and the unapproachable reactors of nuclear power plants, where it is hard to perform non-destructive investigations.

In constructing smart structures, qualitatively high predictions of mechanical behavior are needed. Data that are to be used for these purposes can be acquired through direct *in-situ* experiments or through rigorous numerical techniques. In the field of numerical analysis, finite element analysis is generally accepted. In analyzing civil structures, beam finite elements are widely used due to their simplicity in modeling analysis objects.

Among various smart materials, the piezoelectric materials are being widely considered for adoption in smart structures. In the literature, the 'direct piezoelectric effect' explains the phenomenon of electrical polarization that occurs due to strains caused by applied loads. In this case, an electrical charge is produced on the surface of the material. Conversely, the 'converse piezoelectric effect' indicates the case where strain is produced in the material due to placement of the piezoelectric material within an electric field (Chen *et al.* 2001). By constructing constitutive equations of a material that represents the direct and converse piezoelectric effect, the transduction mechanism between mechanical and electrical energy can be established. The piezoelectric effect has been observed in a number of materials such as natural quartz crystals, polycrystalline piezoceramic, semicrystalline polyvinylidene polymer, and human bone. Among these, lead zirconium titanate (PZT) and polyvinylidene fluoride (PVDF) are generally adopted as mechanically acceptable materials (Clark *et al.* 1998).

After a publication on the finite element analysis of piezoelectric materials by Allik and Hughes (1970), a great deal of research has focused on this subject (Benjeddou 2000). Benjeddou (2000) summarized the formulation, limits of application, and research trends in this field. He discusses some of finite elements such as solid element, shell element, plate element, and beam element, which are already in use. Shen (1995) extends the Hu-Washizu variational principle to formulate a 2-node Timoshenko beam finite element and introduces degrees of freedom for electrical potential. Carpenter (1997) develops an Euler-Bernoulli beam finite element that has degrees of freedom for electrical potential to control axial and bending behaviors of a beam. In addition, some analytical approaches do not include the degrees of freedom for electrical potential. For example, Robbins and Reddy (1991) formulated four different types of layered beam elements based on a thermal analogy approach. The first two equivalent one-layer models are based on classical beam theory and shear-deformation theory. Among the other two multi-layered models, the first one assumes that the axial displacement is interpolated linearly and vertical displacement is constant. The second assumes that the axial and vertical displacements are both interpolated linearly. Accordingly, since material characteristics vary along the thickness, layered modeling is adopted that leads to improved results

of the generated voltage and shear deformation (Robbins *et al.* 1991).

Using the sandwich beam theory, Baz and Ro (1996) formulate a 2-node beam element to construct the ACLD (active constrained-layer damping) beam system where shear deformation of beam and piezoelectric material is ignored (Benjeddou 2000). By comparison, Benjeddou *et al.* (1997, 1999) suggest an extension actuation mechanism where shear deformation is ignored if the piezoelectric material is attached outside of the beam structure. Also suggested is a shear actuation mechanism where shear deformation is taken into account if the piezoelectric material is attached inside the beam structure. Smyser and Chandrashekhara (1997), Surace *et al.* (1997), Aldraihem *et al.* (1997) develop a 2-node beam element based on the Timoshenko and Euler-Bernoulli beam theories. Lesieutre and Lee (1996) develop a 3-node beam element where the second order shape function is used for interpolation of the axial and shear deformations, and the third order Hermitian function is used in case of the vertical displacement. Lin *et al.* (2000) derive an analytical solution to the elastic beam with the piezoelectric layer under the electric field and present the explicit expressions of its displacement and stress.

In this study, a new smart beam finite element is proposed for numerical modeling of a beam with bonded plate-type piezoelectric sensors and actuators. Constitutive equations for the direct piezoelectric effect and converse piezoelectric effect are also developed. By using the variational principle, the equations of motion for the smart beam finite element are derived. The proposed 2-node beam finite element is an isoparametric element based on Timoshenko beam theory. Formulation of the isoparametric element that is based on Timoshenko beam theory is clear and concise and accuracy of results is verified. Validity of the proposed element is shown through comparing analytical results of the verification examples with those used by previous researchers. Through adoption of smart beam finite elements, it is possible to simulate control of structural behavior by applying voltage to piezoelectric actuators, and also to monitor structural behavior by sensing voltage of the piezoelectric sensors.

2. Timoshenko beam theory

In order to consider the effect of shear deformation, a displacement field based on the Timoshenko beam theory is assumed (Fig. 1). A general summary of Timoshenko beam theory is given as follows (Owen *et al.* 1980). The plane normal to the neutral axis remains straight after deformation, but it need not remain normal to the neutral axis. The axial displacement $\bar{u}$ at an arbitrary point (x, z) can be expressed by the rotational displacement $\theta(x)$ at the normal plane

$$\bar{u}(x, z) = -z\theta(x) \tag{1}$$
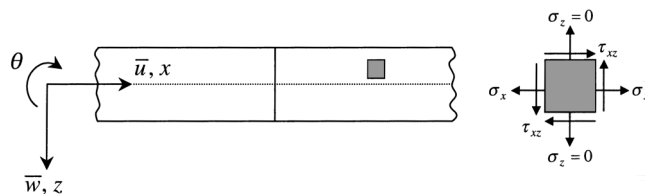
Fig. 1 Timoshenko beam

Taking into account shear deformation β, the rotational displacement is

$$\theta(x) = \frac{dw}{dx} - \beta \tag{2}$$

Vertical displacement $\overline{w}$ at an arbitrary point (x, z) is given as the vertical displacement of the neutral axis.

$$\overline{w}(x) = w(x) \tag{3}$$

Axial strain that is based on infinitesimal deformation theory can be expressed as

$$\varepsilon_x = \frac{\partial \overline{u}}{\partial x} = -z\frac{d\theta}{dx} \tag{4}$$

And, it is also possible to obtain the shear strain as

$$\gamma_{xz} = \frac{\partial \overline{u}}{\partial z} + \frac{\partial \overline{w}}{\partial x} = -\theta + \frac{dw}{dx} = \beta \tag{5}$$

3. Formulation of smart beam finite element

When piezoelectric materials are attached to beam structures, they can function as sensors and actuators. If electric currents are applied to a piezoelectric actuator, loads that are produced by the inverse piezoelectric effect of the piezoelectric materials are applied to the structure. Conversely, if strains in the piezoelectric sensor are produced by external loads, a magnetic field is generated by the direct piezoelectric effects of the material. In this section, formulation of a smart beam finite element that is used in modeling beam-type smart structures with a piezoelectric sensor and actuator is given (Fig. 2).

To derive equations of motion for the piezoelectric sensor and piezoelectric actuator, some assumptions are posed as follows (Lin and Huang 1999): (1) The thickness of piezoelectric sensor and the piezoelectric actuator is very thin relative to that of the beam structure itself. (2) The piezoelectric material is polarized toward the positive direction of the z-axis. (3) When a magnetic field is introduced, only axial load in the direction of x-axis is generated. (4) The distribution of electrodes runs parallel (Fig. 3). (5) The piezoelectric material is homogeneous and isotropic, and it has linear elastic behavior.

To derive the kinetic equations of the beam structures, the following assumptions must be posed. (1) The behavior of the beam structure can be adequately expressed by vertical and rotational displacement, and axial displacement is small enough to be ignored. (2) Shear deformation is based on the Timoshenko beam theory. (3) Axial stress σ_x and shear stress τ_{xz} are considered. (4) The piezoelectric material is perfectly bonded to the beam structure. (5) The piezoelectric sensor, the piezoelectric actuator and the beam structure are modeled as layered materials.

3.1 Determination of the neutral axis

Since the smart beam finite element is constructed in layered type, the location of neutral axis can be evaluated as the following equation.
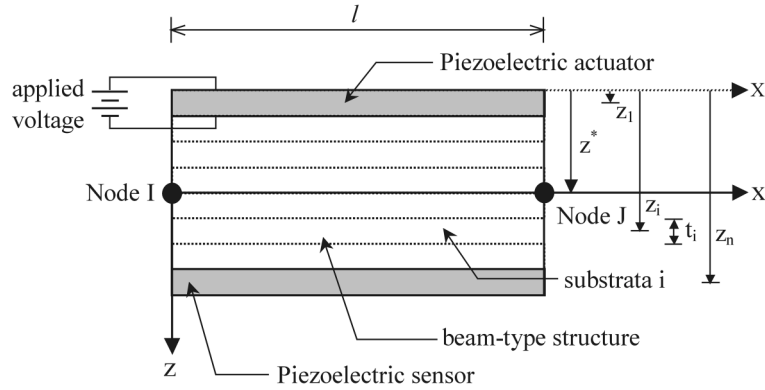
Fig. 2 Smart beam finite element

$$z^* = \frac{\sum_{i=1}^{n} E_i z_i b_i t_i}{\sum_{i=1}^{n} E_i b_i t_i} \tag{6}$$

where E_i, b_i, t_i are elastic modulus, width and thickness of the i-th layer, respectively, and z_i is the distance from top surface to the center of the i-th layer (Fig. 2).

3.2 Constitutive equations of piezoelectric materials

The relations of axial stress-strain-electric field for the piezoelectric actuator can be expressed as follows (Allik and Hughes 1970, Ha *et al*. 1992, Ray *et al*. 1994, Carpenter 1997, Chen *et al*. 1997, Clark *et al*. 1998, Lin and Huang 1999):

$$\sigma_x = E\varepsilon_x - Ed'_{31}e_z \tag{7}$$

where E is the elastic modulus under constant electric field, d'_{31} is the piezoelectric strain constant defined at the local coordinate x-z of the beam element, and e_z is the applied electric field in the z-direction.

Shear stress-shear strain relationship for the piezoelectric actuator is

$$\tau_{xz} = G\gamma_{xz} \tag{8}$$

where the shear modulus of elasticity is $G = E/(2(1+v))$ and v is Poisson's ratio.

The electrical displacement-strain-electric field is assumed to have the following form:

$$D_z = \mu_z^s e_z + e'_{31}\varepsilon_x = (\mu_z^\sigma - Ed_{31}'^2)e_z + Ed'_{31}\varepsilon_x \tag{9}$$

where D_z is the electrical displacement, e_z is the electric field, μ_z^s is the permeativity constant at the constant strain condition, e'_{31} is the piezoelectric stress constant, and μ_z^σ is the permeativity constant for a constant-stress condition.

3.3 Application of variational principle

Modifying the general form of the variational equation for a finite element, it is possible to derive the following variational form (Allik and Hughes 1970, Ray *et al.* 1994).

$$\iiint_V \{ \delta u \rho \ddot{u} \} dv + \iiint_V \{ \delta \varepsilon_x \sigma_x + \delta \beta \tau_{xz} \} dv - \iiint_V \{ \delta e_z D_z \} dv - \delta u P + \iint_{S_1} \delta \phi_1 \overline{\sigma}_1 ds = 0 \quad (10)$$

where ρ is the mass density, ϕ_1 is the electric potential of a piezoelectric actuator, $\overline{\sigma}_1$ is the surface charge of a piezoelectric actuator, u is the displacement of a beam, P is the external load applied to a beam, S_1 is the surface area where electric charge is applied, and V is the volume of a beam.

Substituting Eqs. (5)~(9) into Eq. (10) and referring to Fig. 2, the following variational equation can be derived.

$$\int_0^l \{ \delta u \rho A \ddot{u} \} dx + \int_0^l \left\{ \frac{d(\delta \theta)}{dx} EI \frac{d\theta}{dx} \right\} dx + \int_0^l \{ \delta \beta G \hat{A} \beta \} dx - \int_0^l \left\{ \frac{d(\delta \theta)}{dx} Ed'_{31} Q_p^1 \frac{\partial \phi_1}{\partial z} \right\} dx$$

$$- \int_0^l \left\{ \frac{d(\delta \theta)}{dx} Ed'_{31} Q_p^n \frac{\partial \phi_n}{\partial z} \right\} dx - \int_0^l \left\{ \frac{\partial(\delta \phi_1)}{\partial z} Ed'_{31} Q_p^1 \frac{d\theta}{dx} \right\} dx$$

$$- \int_0^l \left\{ \frac{\partial(\delta \phi_n)}{\partial z} Ed'_{31} Q_p^n \frac{d\theta}{dx} \right\} dx - \int_0^l \left\{ \frac{\partial(\delta \phi_1)}{\partial z} \mu_z^s A_p^1 \frac{\partial \phi_1}{\partial z} \right\} dx$$

$$- \int_0^l \left\{ \frac{\partial(\delta \phi_n)}{\partial x} \mu_z^s A_p^n \frac{\partial \phi_n}{\partial z} \right\} dx - \delta u P + \int_0^l \delta \phi_1 \overline{\sigma}_1 b_1 dx = 0 \quad (11)$$

where the superscripts 1 and n mean the layer number of the piezoelectric actuator and the piezoelectric sensor, respectively, and the specific terms used in Eq. (11) can be obtained as follows considering the contributions of each layer:

$$\rho A = \sum_{i=1}^n \rho_i b_i t_i, \quad EI = \sum_{i=1}^n \left(\frac{E_i b_i t_i^3}{12} + E_i z_i^2 b_i t_i \right), \quad G\hat{A} = \frac{5}{6} \sum_{i=1}^n G_i b_i t_i$$

$$Q_p^1 = z_1 b_1 t_1, \quad Q_p^n = z_n b_n t_n, \quad A_p^1 = b_1 t_1, \quad A_p^n = b_n t_n \quad (12)$$

3.4 Expressions for fields of displacements and electric potentials

Using assumed shape functions of the beam finite element and nodal values of displacement, the displacement fields can be expressed as

$$w(x) = N_1 w_1 + N_2 w_2$$
$$\theta(x) = N_1 \theta_1 + N_2 \theta_2 \quad (13)$$

where each shape function has the form of $N_1 = (l-x)/l, N_2 = x/l$.

The distributions of electric potentials in the piezoelectric actuator and piezoelectric sensor can be assumed by the following functions. The distribution of electric potential in the y direction is
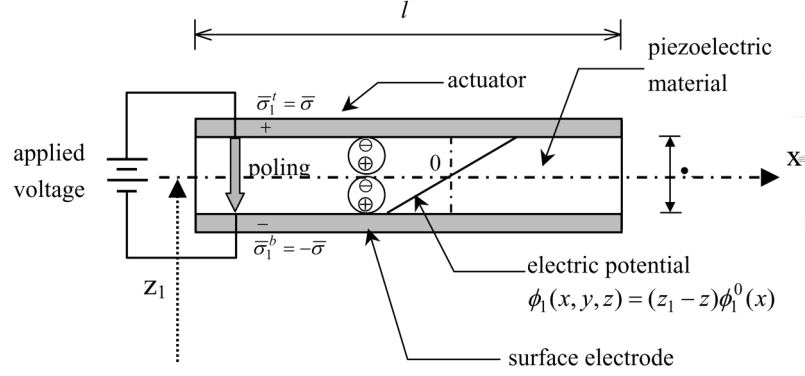
Fig. 3 Electrical actuating model

assumed to be constant (Ray *et al*. 1994) (Fig. 3).

$$\phi_1(x, y, z) \;=\; (z_1 - z)\,\phi_1^0(x)$$

$$\phi_n(x, y, z) \;=\; (z_n - z)\,\phi_n^0(x) \tag{14}$$

The fields of electric potentials for the actuator and sensors, $\phi_1^0(x)$ and $\phi_n^0(x)$, can be interpolated from nodal values as follows:

$$\phi_1^0(x) \;=\; N_1\phi_{11}^0 + N_2\phi_{12}^0$$

$$\phi_n^0(x) \;=\; N_1\phi_{n1}^0 + N_2\phi_{n2}^0 \tag{15}$$

4. Derivation of equations of motion

4.1 Construction of system matrices

Substitution of Eqs. (12)~(15) into Eq. (11) leads to equations of motion that consist of a mass matrix, stiffness matrix, piezoelectric matrix, and a load vector (see Appendix).

In this process, the various relationships are defined as follows:

(1) Curvature-displacement relationships:

$$\varepsilon_f \;=\; -\frac{d\theta}{dx} \;=\; \langle \boldsymbol{B}_f \rangle \{\boldsymbol{u}\} \tag{16}$$

(2) Shear strain-displacement relationships:

$$\varepsilon_s \;=\; \frac{dw}{dx} - \theta \;=\; \langle \boldsymbol{B}_s \rangle \{\boldsymbol{u}\} \tag{17}$$

(3) Electric field-electric potential relationships:

Electric field-electric potential relationships for the piezoelectric actuator and piezoelectric sensor can be expressed as (Ha *et al*. 1992, Ray *et al*. 1994, Chen *et al*. 1997, Lin and Huang 1999)

$$e_z^1 = -\frac{\partial \phi_1}{\partial z} = \langle B_p^1 \rangle \{\varphi_1\} \ ; \ e_z^n = -\frac{\partial \phi_n}{\partial z} = \langle B_p^n \rangle \{\varphi_n\} \tag{18}$$

where $\{\varphi_1\} = \langle \phi_{11}^0 \ \phi_{12}^0 \rangle^T$, $\{\varphi_n\} = \langle \phi_{n1}^0 \ \phi_{n2}^0 \rangle^T$.

4.2 Electrical actuating vector

As shown in Fig. 3, if the distributed applied charge density $\overline{\sigma}$, which is applied on the surface of the piezoelectric actuator, is expressed as voltage (difference of electric potential) and the variation of the electric potential at the surface of piezoelectric actuator is formulated, the electrical actuating vector in each beam finite element can be constructed. The applied surface charge density can be expressed as a function of applied electric voltage as Griffiths (1981), Ray *et al.* (1994)

$$\overline{\sigma} = \frac{\mu_z^s}{t_1} \left\{ \phi_1\left(x, y, z_1 - \frac{t_1}{2}\right) - \phi_1\left(x, y, z_1 + \frac{t_1}{2}\right) \right\} = \frac{\mu_z^s}{t_1} \cdot Voltage \tag{19}$$

where ϕ_1 can be written as a function of x, y, z, i.e., $\phi_1(x, y, z)$.

The variation of the electric potential at the surface of the piezoelectric actuator can be written as follows using Eq. (14).

$$\delta\phi_1^t = (z_1 - z)\delta\phi_1^0(x)\Big|_{z = z_1 - \frac{t_1}{2}} = \frac{t_1}{2}\delta\phi_1^0(x) \ ; \ \delta\phi_1^b = (z_1 - z)\delta\phi_1^0(x)\Big|_{z = z_1 + \frac{t_1}{2}} = -\frac{t_1}{2}\delta\phi_1^0(x) \tag{20}$$

where t and b indicate the top and bottom surfaces of the piezoelectric actuator attached to the upper side of beam structure. With Eqs. (19) and (20), the electrical actuating vector, expressed in terms of the applied electric voltage, can be constructed (see Appendix).

4.3 Equations of motion

Following construction of element system matrices, the equations of motion are written as follows:

$$[M^*]\{\ddot{u}\} + ([K_f] + [K_s])\{u\} - [K_{p11}]\{\varphi_1\} - [K_{pn1}]\{\varphi_n\} = \{P\} \tag{21}$$

$$[K_{p11}]^T\{u\} + [K_{p12}]\{\varphi_1\} = \{Q_1\} \tag{22}$$

$$[K_{pn1}]^T\{u\} + [K_{pn2}]\{\varphi_n\} = \{0\} \tag{23}$$

With static condensation of Eqs. (21), (23), the following simple equation can be constructed.

$$[M^*]\{\ddot{u}\} + [K^*]\{u\} = \{P^*\} \tag{24}$$

where

$$[K^*] = [K_f] + [K_s] + [K_{p11}][K_{p12}]^{-1}[K_{p11}]^T + [K_{pn1}][K_{pn2}]^{-1}[K_{pn1}]^T \tag{25}$$

$$\{P^*\} = \{P\} + [K_{p11}][K_{p12}]^{-1}[Q_1] \tag{26}$$

By assembling the element system matrices, the equation of motion for the entire smart structure is obtained as

$$[M]\{\ddot{U}\} + [C]\{\dot{U}\} + [K]\{U\} = \{F\} \tag{27}$$

where the damping matrix $[C]$ can be simply determined from matrices $[M]$ and $[K]$ if Rayleigh damping is assumed (Cook *et al.* 1989).

4.4 Analysis of voltage

Using Eqs. (22) and (23), the generated voltage can be analyzed from the piezoelectric actuator and piezoelectric sensor. Eqs. (22) and (23), the nodal values of electrical potentials at the piezoelectric actuator and sensor, can be rewritten as:

$$\{\varphi_1\} = [K_{p12}]^{-1}(\{Q_1\} - [K_{p11}]^T\{u\}) \tag{28}$$

$$\{\varphi_n\} = -[K_{pn2}]^{-1}[K_{pn1}]^T\{u\} \tag{29}$$

Thus, using the displacement vector obtained by solution of Eq. (27), the generated voltage of the piezoelectric actuator and piezoelectric sensor can be evaluated as follows:

$$\{V_1\} = t_1\{\varphi_1\} \tag{30}$$

$$\{V_n\} = t_n\{\varphi_n\} \tag{31}$$

4.5 Control of free vibration: Constant-gain feedback control

As shown in Fig. 4, the beam structure equipped with piezoelectric devices can be constructed. The piezoelectric actuator layer and piezoelectric sensor layer are attached to the main beam structure. As the beam vibrates, voltage is produced in the piezoelectric sensor layer, and the amplified voltage is transferred to the piezoelectric actuator. If upward vertical displacement at the tip occurs, tensile strain is produced in the piezoelectric sensor layer. Therefore, the feedback voltage produces tensile strain in the piezoelectric actuator resulting in the control of vibration.
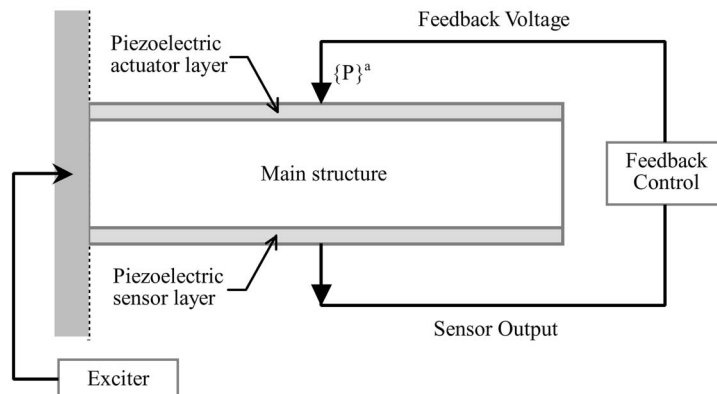

Fig. 4 Smart beam structure with piezoelectric sensor and actuator
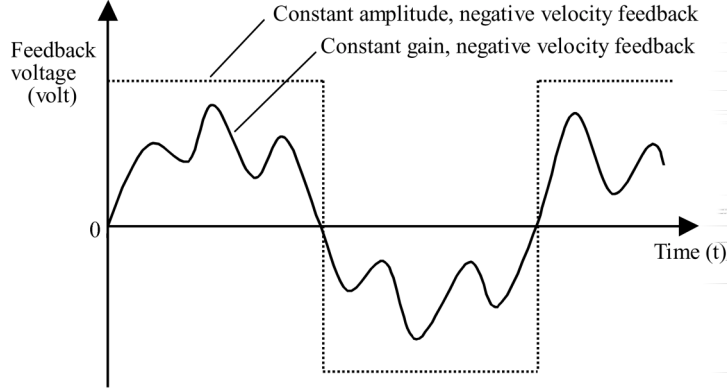
Fig. 5 Evaluation of feedback voltage

For vibration control of beam structures, an efficient control algorithm is needed. The control force generated by the feedback voltage contributes to reduce the amplitude of the vibration as a damping force. Among various control schemes such as constant-gain feedback control and constant-amplitude feedback control and so on, constant-gain feedback control scheme is adopted in this study (Fig. 5).

As seen in Eq. (26), the load term is divided into two parts: externally applied load and electrically generated load. The electrically generated load serves as a feedback voltage load to actively control a smart beam structure. Similar to the electrically generated load in Eq. (26), the control force can be given as follows:

$$\{\boldsymbol{P}^e\} = -[\boldsymbol{K}_{p11}][\boldsymbol{K}_{p12}]^{-1}\{\boldsymbol{Q}^e\} \tag{32}$$

where $\{\boldsymbol{P}^e\}$ is electrically generated feedback load and $\{\boldsymbol{Q}^e\}$ represents an electrical actuating vector evaluated based on the voltage measured from the piezoelectric sensor. Following the theory of negative velocity feedback control, the electric actuating vector $\{\boldsymbol{Q}^e\}$ can be constructed as follows (Peng *et al*. 1998):

$$\{\boldsymbol{Q}^e\} = -G \cdot \left(\mu_z^s \cdot b_1 \cdot \frac{L}{2}\right)\{\dot{\boldsymbol{Q}}_n\} = G \cdot t_n \cdot \left(\mu_z^s \cdot b_1 \cdot \frac{L}{2}\right)\left(\mu_z^s \cdot b_n \cdot \frac{L}{2}\right)[\boldsymbol{K}_{pn2}]^{-1}[\boldsymbol{K}_{pn1}]^T\{\dot{\boldsymbol{u}}\} \tag{33}$$

where G is feedback gain and has constant value; therefore, the scheme is called as constant-gain feedback scheme. From Eqs. (32) and (33), the electrically generated loading term is determined as

$$\{\boldsymbol{P}^e\} = -G \cdot t_n \cdot \left(\mu_z^s \cdot b_1 \cdot \frac{L}{2}\right)\left(\mu_z^s \cdot b_n \cdot \frac{L}{2}\right)[\boldsymbol{K}_{p11}][\boldsymbol{K}_{p12}]^{-1}[\boldsymbol{K}_{pn2}]^{-1}[\boldsymbol{K}_{pn1}]^T\{\dot{\boldsymbol{u}}\} \tag{34}$$

With substitution of Eq. (34), Eq. (24) is arranged as follows:

$$[\boldsymbol{M}^*]\{\ddot{\boldsymbol{u}}\} + [\boldsymbol{C}^*]\{\dot{\boldsymbol{u}}\} + [\boldsymbol{K}^*]\{\boldsymbol{u}\} = \{\boldsymbol{P}\} \tag{35}$$

where

$$\{\boldsymbol{C}^*\} = G \cdot t_n \cdot \left(\mu_z^s \cdot b_1 \cdot \frac{L}{2}\right)\left(\mu_z^s \cdot b_n \cdot \frac{L}{2}\right)[\boldsymbol{K}_{p11}][\boldsymbol{K}_{p12}]^{-1}[\boldsymbol{K}_{pn2}]^{-1}[\boldsymbol{K}_{pn1}]^T \tag{36}$$

As a consequence, by applying the law of negative velocity feedback control, the equations of motion for the entire smart beam structure can be written as,

$$[M]\{\ddot{U}\} + [C + C^e]\{\dot{U}\} + [K]\{U\} = \{F\} \tag{37}$$

where matrix $[C^e]$ represents the damping effect improved by the control force.

5. Numerical examples

Numerical analyses of several examples are performed to show accuracy and efficiency of the smart beam finite element, and to verify the capability of free vibration control using the smart beam finite element.

5.1 Piezoelectric PVDF bimorph cantilever beam

As an example of numerical analysis, the piezoelectric PVDF bimorph cantilever beam is chosen (Fig. 6). Material properties for PVDF are shown in Table 1 and the beam is modeled with five smart beam finite elements that have the same length. The piezoelectric PVDF bimorph beam is constructed with two PVDF layers and each layer is polarized in the opposite direction.
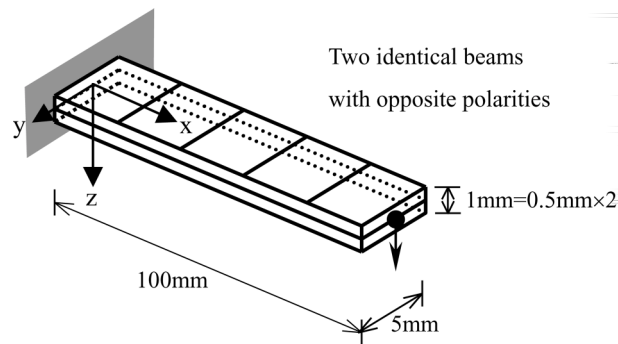
E_p=2E9(N/m^2), ν_p=0.29,

$d_{31}{}'$=2.2E-11(m/V), μ_z^s=0.1062E-9(F/m)

Fig. 6 Piezoelectric PVDF bimorph cantilever

Table 1 Material properties data

| Materials		PVDF	PZT	Aluminum
	E	2.0×10^9 (N/m^2)	6.3×10^{10} (N/m^2)	7.3×10^{10} (N/m^2)
	Poisson's ratio	0.29	0.35	0.3
Properties	ρ	1800 (kg/m^3)	7600 (kg/m^3)	2630 (kg/m^3)
	d_{31}'	2.2×10^{-11} (C/N)	3.7×10^{-10} (C/N)	-
	μ_z^s	1.062×10^{-10} (F/m)	1.393×10^{-8} (F/m)	-
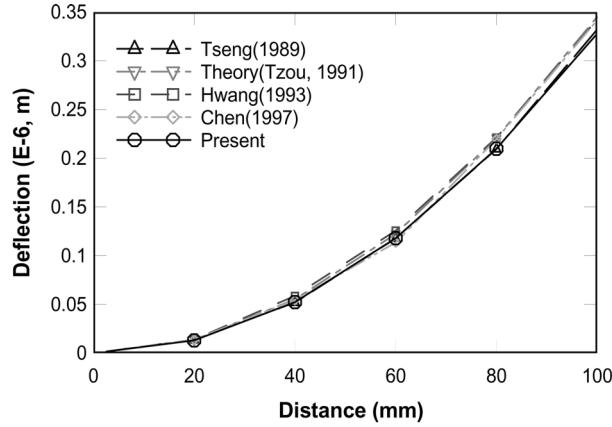
Fig. 7 Comparison of vertical displacement (applied voltage : 1V)

Table 2 Vertical displacement of piezoelectric bimorph cantilever($\times 10^{-6}$ m) (applied voltage: 1V)

	Position (mm)	20	40	60	80	100
	Theory (Tzou 1991)	0.140	0.552	1.224	2.208	3.451
	Tzou (1991)	0.124	0.508	1.160	2.100	3.300
Analyses	Shen (1995)	0.132	0.528	1.188	2.112	3.300
	Chen (1997)	0.139	0.547	1.135	2.198	3.416
	Present	0.131	0.524	1.180	2.098	3.278

Table 3 Vertical displacement of piezoelectric bimorph cantilever ($\times 10^{-4}$ m)

	Voltage	50	100	150	200
	Theory (Tzou 1991)	0.1725	0.3451	0.5175	0.6900
Analyses	Chen (1997)	0.1755	0.3409	0.5067	0.6819
	Present	0.1639	0.3278	0.4916	0.6555
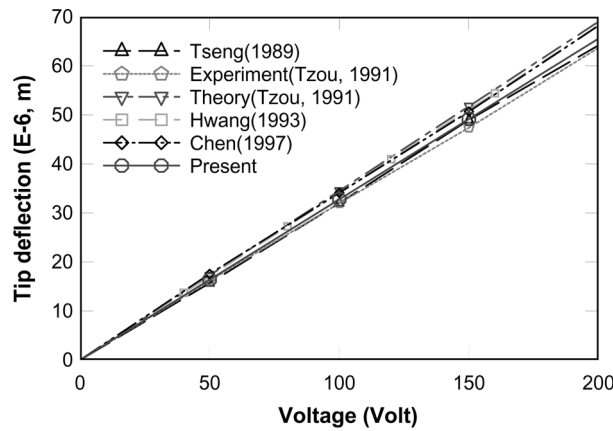
Fig. 8 Vertical displacement due to varying voltage

Table 4 Comparison of numbers of degrees of freedom

	Models	No. of nodal points	Degrees of freedom		
			Structural	Electrical	Total
Analyses	Tseng (1989)	36	108	36	144
	Hwang (1993)	12	36	5	41
	Shen (1995)	6	48	12	60
	Chen (1997)	12	36	12	48
	Present	6	18	12	30
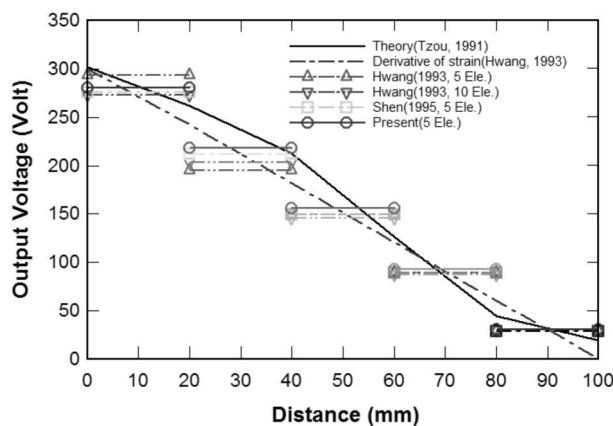
Fig. 9 Generated voltages (Tip displacement : 1 cm)

As a result of an applied voltage, tensile or compressive forces are generated in each layer, which result in bending of the beam. Conversely, a voltage is generated if artificial deformation of the beam occurs. Analytical results of this study are compared with those of the previous studies. Vertical displacements in each node of the beam that resulted from the actual voltage are compared in Fig. 7 and Table 2. In Table 3 and Fig. 8 vertical displacement at the end of the beam is compared for voltages between 0 V to 200 V. The numbers of structural degrees of freedom, electric degrees of freedom, and total degrees of freedom are shown in Table 4. When compared with the results of previous studies, it is noted that the proposed element gives accurate and efficient results with fewer structural and electric degrees of freedom.

5.2 The aluminum cantilever beam with the PZT piezoelectric sensor

An aluminum cantilever beam with six pairs of PZT piezoelectric sensors (Fig. 10) is chosen as a second example (Shen 1995). The PZT piezoelectric sensors are symmetrically attached to the aluminum cantilever. Material constants are also shown in Table 1.

When vertical displacement at the right end reaches 0.47625 cm, the generated voltage in each pair of the piezoelectric sensors is analyzed and compared with the result of Shen (1995). As shown in Table 5, results indicate good agreement with those of the Shen (1995), and show only a discrepancy of from 2% to 4% with those of the experiment.
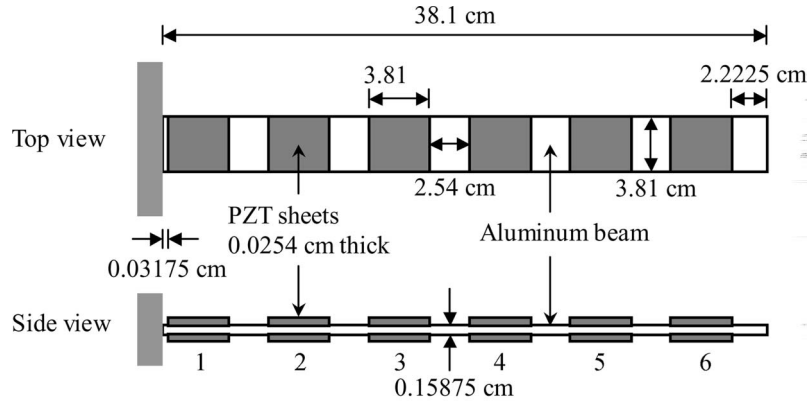
Fig. 10 Aluminum cantilever beam with PZT piezoelectric sensors

Table 5 Voltage in the piezoelectric sensors

Piezoelectric sensor		1	2	3	4	5	6
	Specimen 1	11.0	8.8	7.26	-	-	-
	Specimen 2	11.5	8.4	7.23	-	-	-
	Specimen 3	11.25	8.9	7.25	-	-	-
Shen (1995)	Analytic	10.98	9.04	7.10	5.15	3.20	1.26
	Error (%) (experiment)	2.4	3.8	1.9	-	-	-
Present	Analytic	11.01	9.06	7.11	5.17	3.22	1.27
	Error (%) (experiment)	2.1	4.0	1.9	-	-	-

5.3 Free vibration control of the beam structure

The size and shape of a third set of example structures are shown in Fig. 11. In the analysis, a simply supported 1-span beam (40 m) and continuous 3-span beam (3 @ 25 m) are taken as
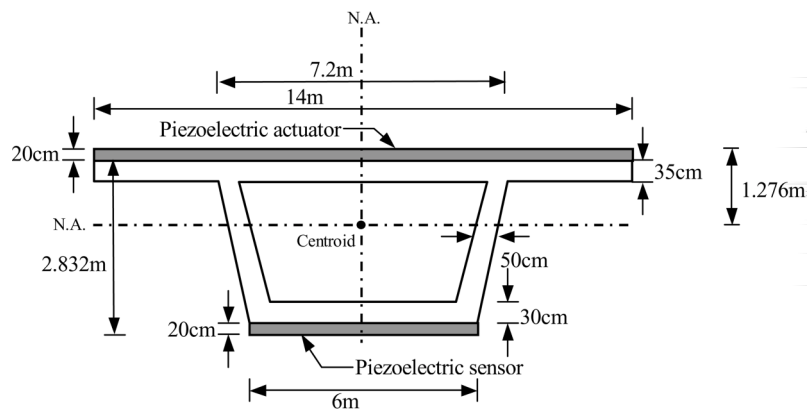
Fig. 11 Sectional view of example structure

Table 6 Sectional and material properties

Section properties	Area (m^2)	5.922	
	Inertia moment (I_z, m^4)	17.157	
	Materials	Concrete	PZT
Properties	E (N/m^2)	3.532×10^{10}	6.3×10^{10}
	v	0.2	0.3
	μ_z^s (F/m)	-	1.3×10^{-8}
	ρ (kg/m^3)	4812	7600
	d_{31}' (m/V)	-	1.9×10^{-10}
	Damping ratio (%)	5	
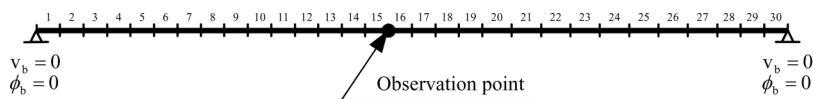
(a) Simple one span beam
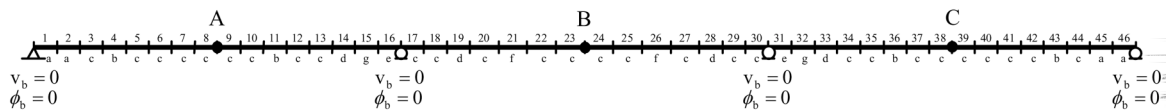
(b) 3-span continuous beam

Fig. 12 Finite element mode

numerical examples. The sectional properties are assumed to be constant along the overall length of the beam structure. The piezoelectric actuator and sensor are manufactured with PZT and the sectional and material properties are given in Table 6. As shown in Fig. 12, the simple one-span beam is modeled with 30 smart beam finite elements and the 3-span continuous beam is modeled with 46 beam finite elements.

5.3.1 Simply supported 1-span beam

The free vibration is exerted by the initial rotational displacement of 1.0 radian at the center of the span. The variation of vertical displacement is investigated for a gain that varies from 0 to 4,000. As indicated in Fig. 13, the reduction of the vertical displacement due to the control force resulting from the piezoelectric effect is prominent when the gain is 4,000. This is due to the control force, which is generated by the voltage at the piezoelectric actuator and which is the electrical actuating bending moment acted in the beam structure as given in Fig. 14. As the vibration is reduced and controlled, the magnitude of the control force reduces with time. In Fig. 15, the frequency content is shown as a function of gain. As shown in the figures, a decrease in the frequency content occurs as the magnitude of the gain is increased.
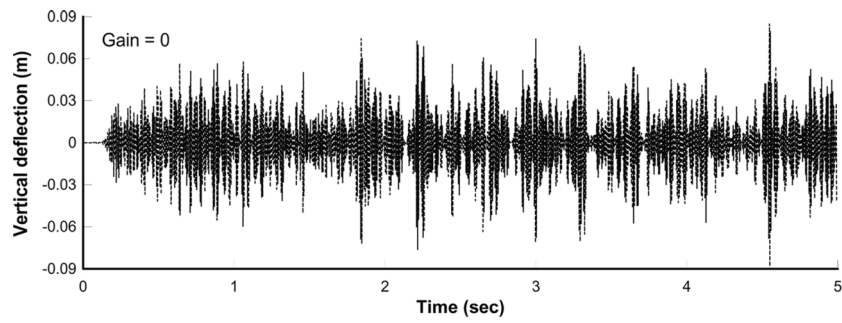
(a) Gain = 0
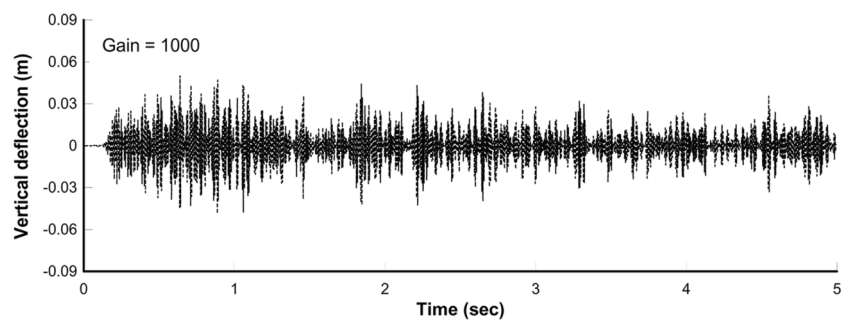
(b) Gain = 1000
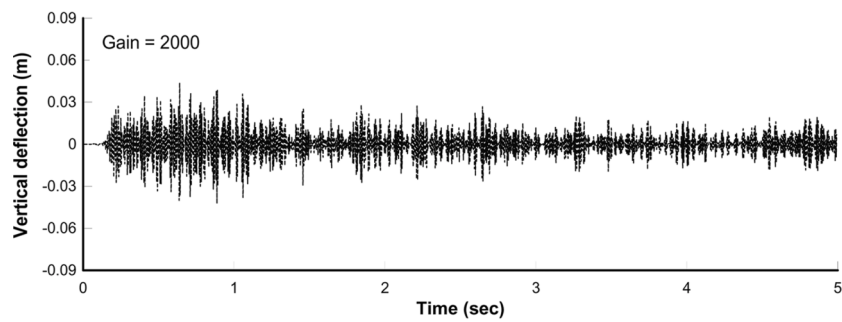
(c) Gain = 2000
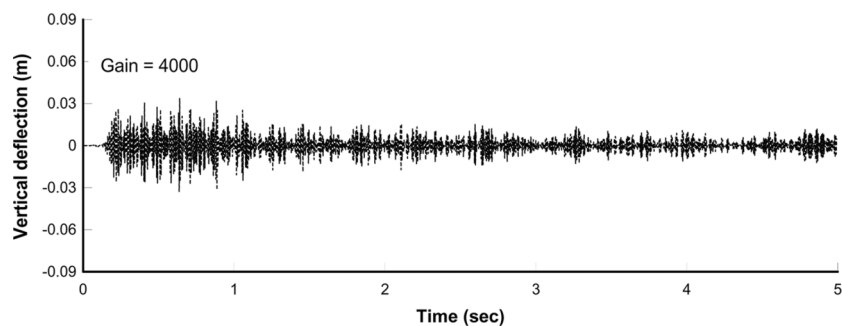
(d) Gain = 4000

Fig. 13 Vertical displacement at the center of span

(a) Gain = 1000

(b) Gain = 2000


(c) Gain = 4000
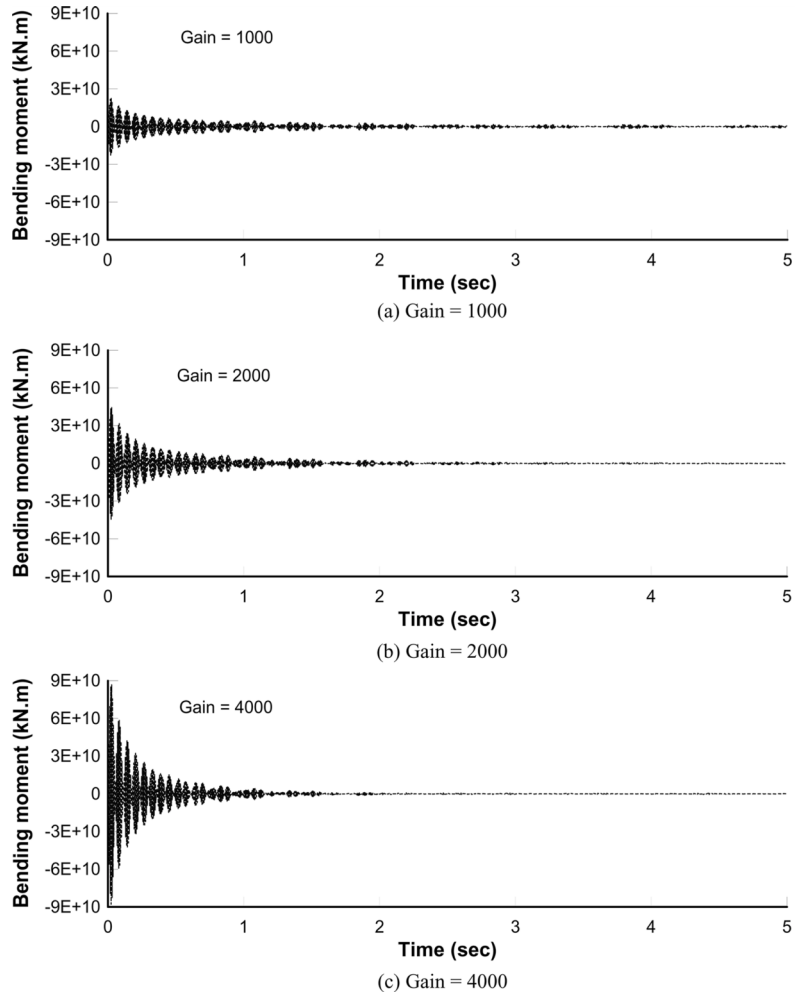
Fig. 14 Electrical actuating moment at the center of span
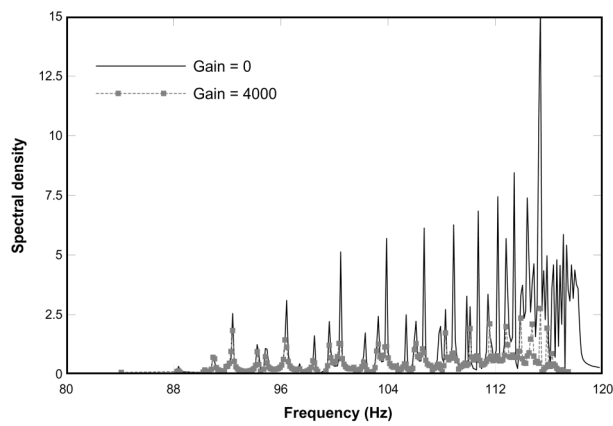
Fig. 15 Frequency contents of vertical displacement
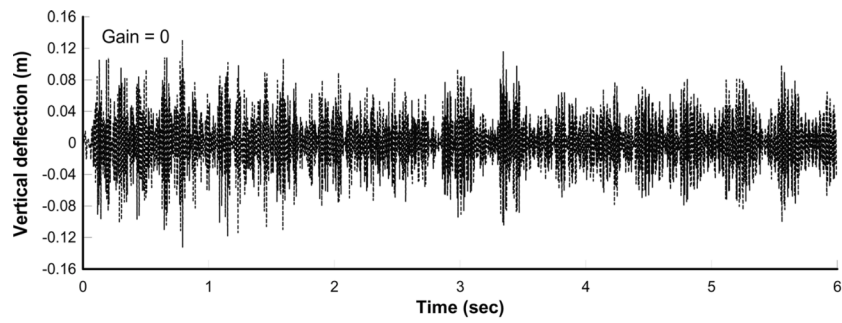
(a) Gain = 0
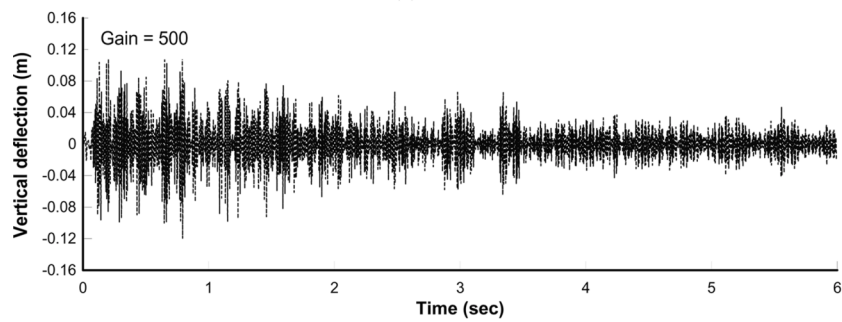
(b) Gain = 500
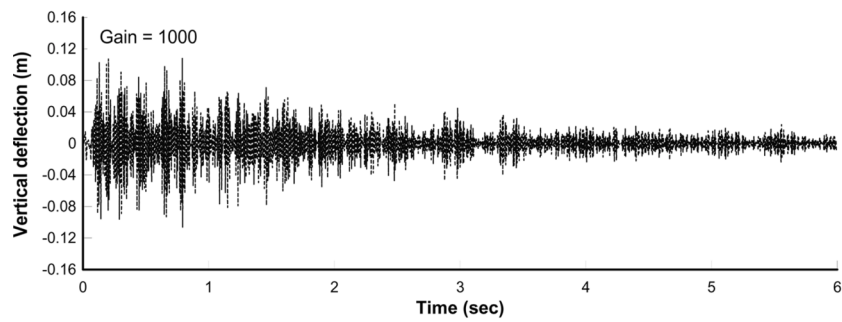
(c) Gain = 1000
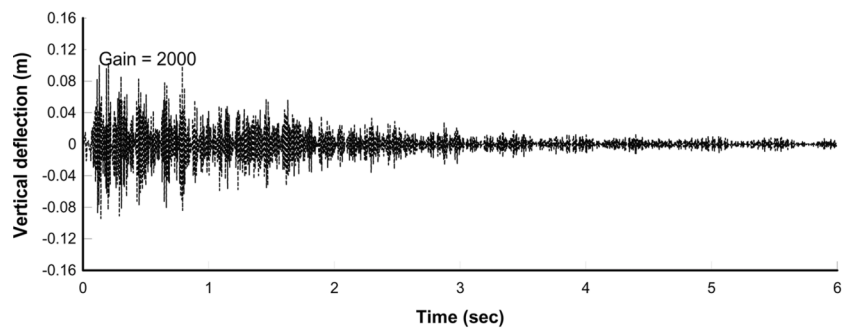
(d) Gain = 2000

Fig. 16 Vertical displacement at the center of the first span (point A)
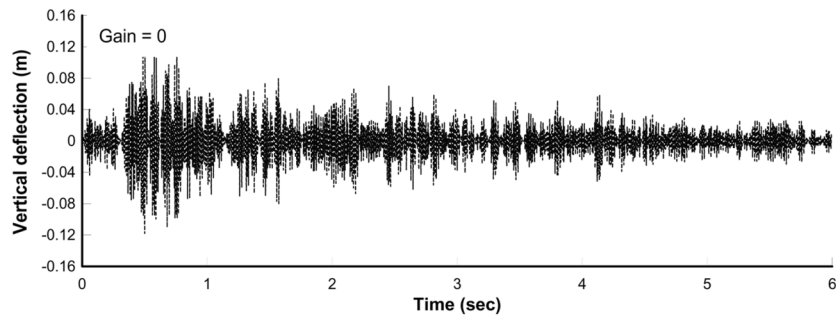
(a) Gain = 0
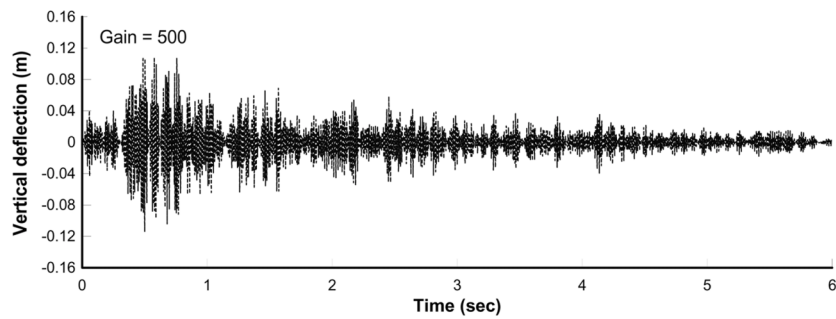
(b) Gain = 500
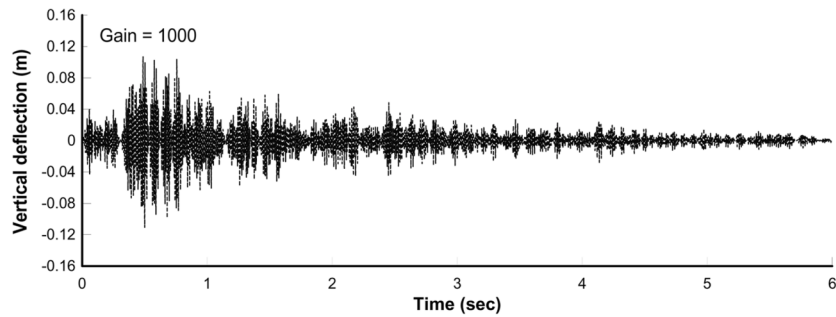
(c) Gain = 1000
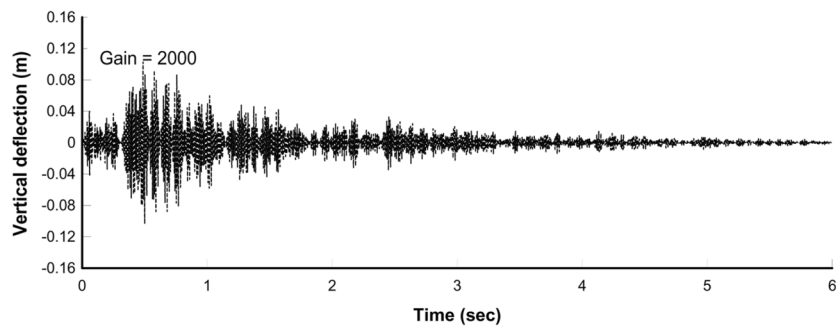
(d) Gain = 2000

Fig. 17 Vertical displacement at the center of the center span (point B)

(a) Gain = 500

(b) Gain = 1000

(c) Gain = 2000
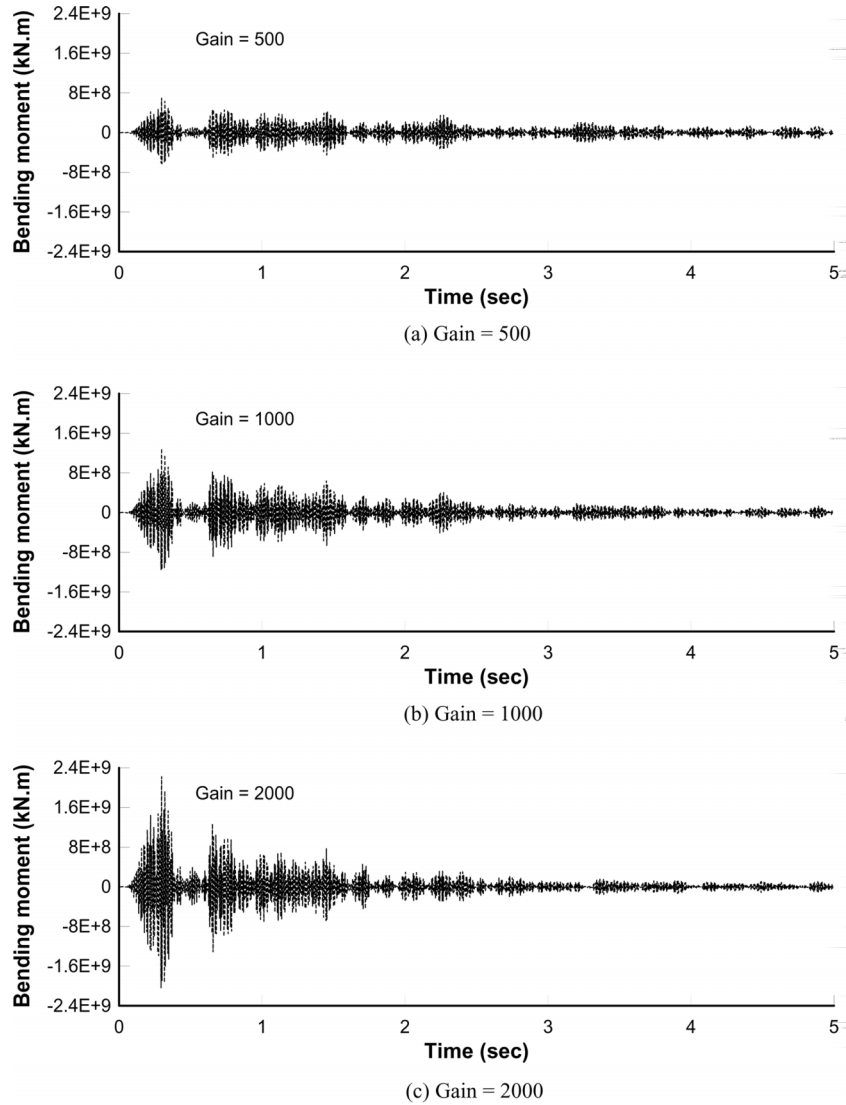
Fig. 18 Electrical actuating moment at the center of the first span (point A)

5.3.2 Continuous 3-span beam

In this analysis, free vibration is obtained by imposing an initial rotational displacement of 1.0 radian at the center of central span. The change in the vertical displacement in the free vibration is investigated by varying the gain between 0 and 2,000. As shown in Figs. 16 and 17, as the gain is increased the vertical displacements at the center of each span are controlled efficiently. Similar to the case of the previous simply supported 1-span beam, the electrical actuating moment serves as the control force (Figs. 18 and 19). Fig. 20 also shows a decrease in the frequency content as the gain is increased.

(a) Gain = 500

(b) Gain = 1000

(c) Gain = 2000
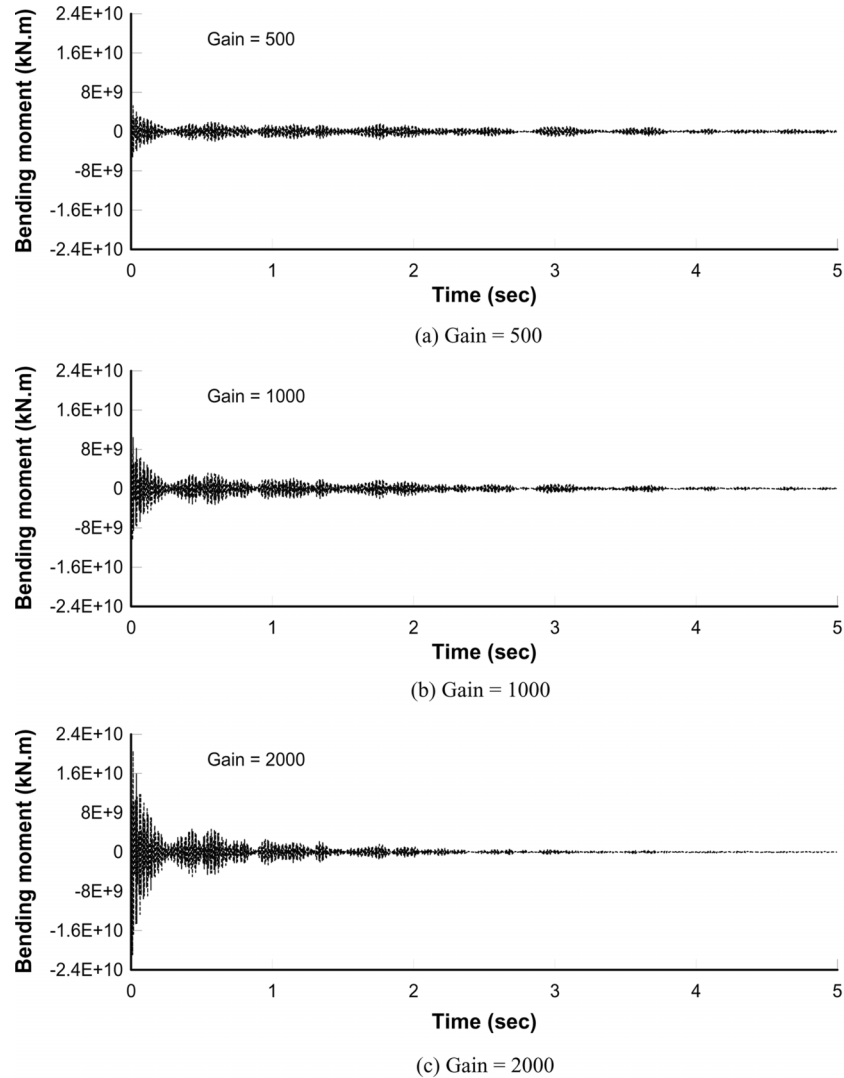
Fig. 19 Electrical actuating moment at the center of the center span (point B)

6. Conclusions

In this study, a new smart beam finite element based on Timoshenko beam theory is proposed for analysis of a beam-type smart structure with bonded plate-type piezoelectric sensors and actuators. By modifying the general variational principle for the formulation of a finite element, equations of motion for the smart beam finite element are derived. The validity of the proposed element is shown through comparing analytical results of a PVDF bimorph cantilever beam and an aluminum cantilever beam that has a PZT sensor with those of other previous researchers.

With use of a smart beam finite element, it is possible to simulate free vibration control by sensing the voltage of the piezoelectric sensors and applying the voltages to the piezoelectric
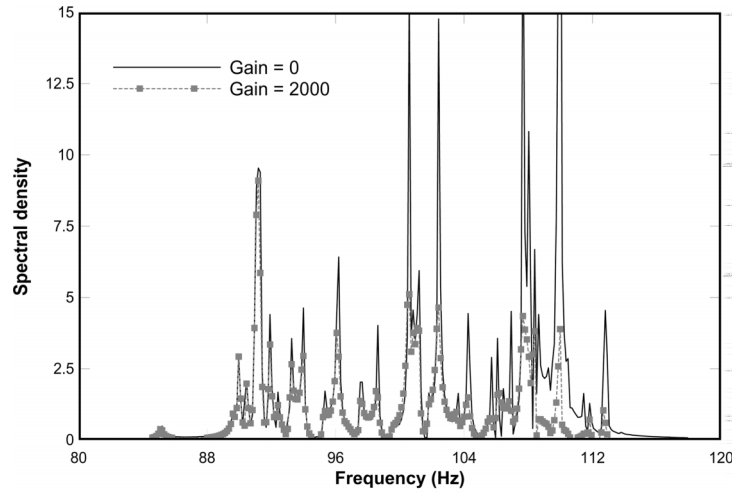
(a) Center point of first span (point A)
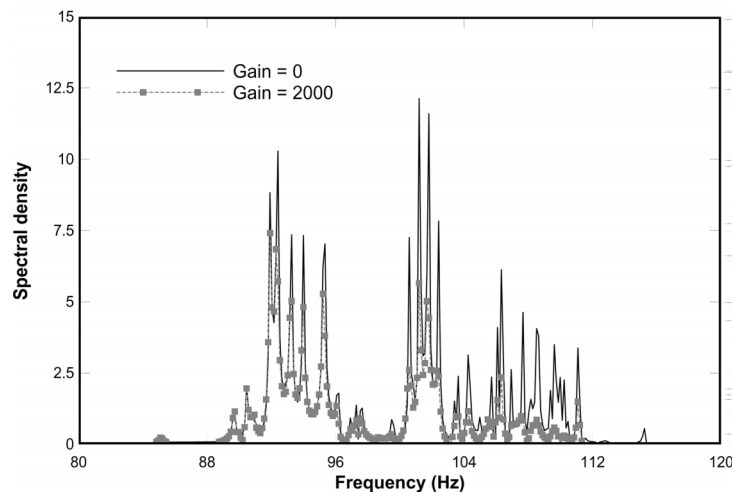
(b) Center point of center span (point B)

Fig. 20 Frequency contents of vertical displacement at the center of span

actuators. For verification, a simply supported 1-span beam and a continuous 3-span beam are analyzed as numerical examples. Through the example analyses it is noted that by applying the scheme of estimating the voltage given to piezoelectric actuator from the voltage of piezoelectric sensor, it is possible to simulate active control of free vibration of the beam-type structures.

Acknowledgements

References

Aldraihem, O.J., Wetherhold, R.C. and Singh, T. (1997), "Distributed control of laminated beams: Timoshenko theory vs. Euler-Bernoulli theory", *J. Intelligent Mat. Sys. Struct.*, **8**, 150-157.

Allik, H. and Hughes, T.J.R. (1970), "Finite element method for piezoelectric vibration", *Int. J. Numer. Meth. Eng.*, **2**, 151-157.

Baz, A. and Ro, J. (1996), "Vibration control of plates with active constrained layer damping", *Smart Mater. Struct.,* **5**, 272-280.

Benjeddou, A., Trindade, M.A. and Ohayon, R. (1997), "A unified beam finite element model for extension and shear piezoelectric actuation mechanisms", *J. Intelligent Mat. Sys. Struct.,* **8**, 1012-1025.

Benjeddou, A., Trindade, M.A. and Ohayon, R. (1999), "New shear actuated smart structure beam finite element", *AIAA J.,* **37**(3), 378-383.

Benjeddou, A. (2000), "Advances in piezoelectric finite element modeling of adaptive structural elements: A survey", *Comput. Struct.,* **76**(1-3), 347-363.

Carpenter, M.J. (1997), "Using energy methods to derive beam finite elements incorporating piezoelectric materials", *J. Intelligent Mat. Sys. Struct.*, **8**, 26-40.

Chen, S.H., Wang, Z.D. and Liu, X.H. (1997), "Active vibration control and suppression for intelligent structures", *J. Sound Vib.*, **200**(2), 167-177.

Chen, S.H., Yao, G.F. and Lian, H.D. (2001), "A new piezoeletric shell element and its application in static shape control", *Struct. Eng. Mech., An Int. J.,* **12**(5), 491-506.

Clark, R.L., Saunders, W.R. and Gibbs, G.P. (1998), *Adaptive Structures: Dynamics and Control*, John Wiley & Sons, Canada.

Cook, R.D., Malkus, D.S. and Plesha, M.E. (1989), *Concepts and Applications of Finite Element Analysis,* 3rd Edition, John Wiley & Sons., USA.

Griffiths, D.J. (1981), *Introduction to Electrodynamics*, Prentice-Hall, USA.

Ha, S.K., Keilers, C. and Chang, F.K. (1992), "Finite element analysis of composite structures containing distributed piezoceramic sensors and actuators", *AIAA J.*, **30**(3), 772-780.

Hughes, T.J.R. (1987), *The Finite Element Method, Linear Static and Dynamic Finite Element Analysis*, Prentice-Hall, USA.

Hwang, W.S. and Park, H.C. (1993), "Finite element modeling of piezoelectric sensors and actuators", *AIAA J.*, **31**(5), 930-937.

Lesieutre, A. and Lee, U. (1996), "A finite element for beams having segmented active constrained layers with frequency-dependent viscoelastics", *Smart Mater. Struct.,* **5**, 615-627.

Lin, C.C. and Huang, H.N. (1999), "Vibration control of beam-plates with bonded piezoelectric sensors and actuators", *Comput. Struct.,* **73**(1-5), 239-248.

Lin, Q.R., Jin, Z.L. and Liu, Z.X. (2000), "An analytical solution to the laminated piezoelectric beam under the electric field", *Struct. Eng. Mech., An Int. J.,* **10**(3), 289-298.

Owen, D.R.J. and Hinton, E. (1980), *Finite Elements in Plasticity: Theory and Practice*, Pineridge Press Limited, UK.

Peng, X.Q., Lam, K.Y. and Liu, G.R. (1998), "Active vibration control of composite beams with piezoelectrics: A finite element model with third order theory", *J. Sound Vib.*, **209**(4), 635-650.

Ray, M.C., Bhattacharyya, R. and Samanta, B. (1994), "Static analysis of an intelligent structure by the finite element method", *Comput. Struct.*, **52**(4), 617-631.

Robbins, D.H. and Reddy, J.N. (1991), "Analysis of piezoelectrically actuated beams using a layer-wise displacement theory", *Comput. Struct.*, **41**(2), 265-279.

Shen, M.H.H. (1995), "A new modeling technique for piezoelectrically actuated beams", *Comput. Struct.*, **57**(3), 361-366.

Smyser, C.P. and Chandrashekhara, K. (1997), "Robust vibration control of composite beams using piezoelectric devices and neural networks", *Smart Mater. Struct.,* **6**, 178-189.

Surace, G., Cardascia, L. and Anghel, V. (1997), "Finite element formulation for piezoelectrically actuated timoshenko beam", *The 7-th Int. Conf. Adapt. Struct. Basel: Technomic,* **6**, 498-507.

Tseng, C.I. (1989), "Electromechanical dynamics of a coupled piezoelectric/mechanical system applied to vibration control and distributed sensing", Ph.D. Dissertation, University of Kentucky, USA.

Tzou, H.S. and Tseng, C.I. (1991), "Distributed vibration control and identification of coupled elastic/piezoelectric systems: Finite element formulation and application", *Mech. Systems Signal Process*, **5**, 215-231.

Appendix: Composition of element matrix

1. Curvature-displacement relationships matrix

$$\langle \boldsymbol{B}_f \rangle = \langle 0 \quad \frac{1}{l} \quad 0 \quad -\frac{1}{l} \rangle \tag{38}$$

where, l stands for length of beam element.

2. Shear strain-displacement relationships matrix

$$\langle \boldsymbol{B}_s \rangle = \langle -\frac{1}{l} \quad -\frac{l-x}{l} \quad \frac{1}{l} \quad -\frac{x}{l} \rangle \tag{39}$$

where, x is coordinate in the local axes system.

3. Electric field-electric potential relationships matrix

$$\langle \boldsymbol{B}_p^1 \rangle = \langle \boldsymbol{B}_p^m \rangle = \langle -\frac{l-x}{l} \quad -\frac{x}{l} \rangle \tag{40}$$

4. Flexural rigidity matrix

$$\int_0^l \left\{ \frac{d(\delta\theta)}{dx} EI \frac{d\theta}{dx} \right\} dx = \int_0^l \langle \boldsymbol{B}_f \rangle^T EI \langle \boldsymbol{B}_f \rangle dx = \frac{EI}{l} \begin{bmatrix} 0 & 0 & 0 & 0 \\ 0 & 1 & 0 & -1 \\ 0 & 0 & 0 & 0 \\ 0 & -1 & 0 & 1 \end{bmatrix} = [\boldsymbol{K}_f] \tag{41}$$

5. Shear rigidity matrix : 1-point Gaussian quadrature (Hughes 1987)

$$\int_0^l \{ \delta\beta G\hat{A}\beta \} dx = \int_0^l \langle \boldsymbol{B}_s \rangle^T G\hat{A} \langle \boldsymbol{B}_s \rangle dx = \frac{G\hat{A}}{l} \begin{bmatrix} 1 & \frac{l}{2} & -1 & \frac{l}{2} \\ \frac{l}{2} & \frac{l^2}{4} & \frac{l}{2} & \frac{l^2}{4} \\ -1 & -\frac{l}{2} & 1 & \frac{l}{2} \\ \frac{l}{2} & \frac{l^2}{4} & \frac{l}{2} & \frac{l^2}{4} \end{bmatrix} = [\boldsymbol{K}_s] \tag{42}$$

6. First piezoelectric matrix of piezoelectric actuator

$$\int_0^l \left\{ \frac{d(\delta\theta)}{dx} Ed_{31}' Q_p^1 \frac{\partial\phi_1}{\partial z} \right\} dx = \int_0^l Ed_{31}' Q_p^1 \langle \boldsymbol{B}_f \rangle^T \langle \boldsymbol{B}_p^1 \rangle dx = Ed_{31}' b_1 t_1 z_1 \begin{bmatrix} 0 & 0 \\ \frac{1}{2} & \frac{1}{2} \\ 0 & 0 \\ -\frac{1}{2} & -\frac{1}{2} \end{bmatrix} = [\boldsymbol{K}_{p11}] \tag{43}$$

7. First piezoelectric matrix of piezoelectric sensor

$$\int_0^l \left\{ \frac{d(\delta\theta)}{dx} Ed_{31}' Q_p^n \frac{\partial\phi_n}{\partial z} \right\} dx = \int_0^l Ed_{31}' Q_p^n \langle \boldsymbol{B}_f \rangle^T \langle \boldsymbol{B}_p^n \rangle dx = Ed_{31}' b_n t_n z_n \begin{bmatrix} 0 & 0 \\ \frac{1}{2} & \frac{1}{2} \\ 0 & 0 \\ -\frac{1}{2} & -\frac{1}{2} \end{bmatrix} = [\boldsymbol{K}_{pn1}] \qquad (44)$$

8. Second piezoelectric matrix of piezoelectric actuator

$$\int_0^l \left\{ \frac{\partial(\delta\phi_1)}{\partial z} \mu_z^s A_p^1 \frac{\partial\phi_1}{\partial z} \right\} dx = \int_0^l \mu_z^s A_p^1 \langle \boldsymbol{B}_p^1 \rangle^T \langle \boldsymbol{B}_p^1 \rangle dx = \mu_z^s b_1 t_1 \begin{bmatrix} \frac{l}{3} & \frac{l}{6} \\ \frac{l}{6} & \frac{l}{3} \end{bmatrix} = [\boldsymbol{K}_{p12}] \qquad (45)$$

9. Second piezoelectric matrix of piezoelectric sensor

$$\int_0^l \left\{ \frac{\partial(\delta\phi_n)}{\partial z} \mu_z^s A_p^n \frac{\partial\phi_n}{\partial z} \right\} dx = \int_0^l \mu_z^s A_p^n \langle \boldsymbol{B}_p^n \rangle^T \langle \boldsymbol{B}_p^n \rangle dx = \mu_z^s b_n t_n \begin{bmatrix} \frac{l}{3} & \frac{l}{6} \\ \frac{l}{6} & \frac{l}{3} \end{bmatrix} = [\boldsymbol{K}_{pn2}] \qquad (46)$$

10. Electrical actuating vector

$$\int_0^l \delta\phi_1 \bar{\sigma}_1 b_1 dx = \int_0^l \delta\phi_1^t \bar{\sigma} b_1 dx + \int_0^l \delta\phi_1^b (-\bar{\sigma}) b_1 dx = \mu_z^s b_1 \cdot Voltage \cdot \left\{ \begin{array}{c} \frac{l}{2} \\ \frac{l}{2} \end{array} \right\} = \{\boldsymbol{Q}_1\} \qquad (47)$$